



A New Model for Image Inpainting for Different Color Spaces

Zainab A. Abdul Kareem^{1,*}, Ahmed K. Al-Jaberi²

Department of Mathematics, College of Science, University of Basrah, Basrah, Iraq.¹, Department of Mathematics, College of Education for Pure Science, University of Basrah, Basrah, Iraq.²

*Corresponding author. Email: zaynab.eali.sci@uobasrah.edu.iq¹

Article information

Article history:

Received : 29/3/2023

Accepted : 11/7/2023

Available online :

Abstract

The newly developed method of inpainting the missing region in digital images that is based on the isotropic model was applied to a variety of color spaces, including XYZ, YCbCr, NTSC, and HSV color spaces. Tests were performed using masks that the researcher had created based on the original (clear) images; these masks range in both size and shape. In order to evaluate the quality of image inpainting, statistical quality metrics such as MSE (Mean Square Error), PSNR (Peak Signal to Noise Ratio), and SSIM (Structural Similarity Index) are utilized. The performance of this method was superior to the state-of-the-art PDEs (partial differential equations) inpainting methods.

Keywords:

image inpainting; isotropic equation; PDE-based inpainting method; color space.

Correspondence:

Author : Zainab A. Abdul Kareem

Email: zaynab.eali.sci@uobasrah.edu.iq

1. INTRODUCTION

The image is one of the best ways to communicate because it contains information that stands out from other methods. Poor storage, device transfers, and other factors may cause these photos to lose some information. Inpainting uses surrounding information to fill in missing regions [1] [2]. Binary, grayscale, and color images exist[3]. TVs and monitors display color images. Primary and secondary colors are the norm. Red, green, and blue are the primary colors of light, which can be mixed to create secondary colors like magenta, yellow, and cyan [4] [5]. Many color spaces are mathematical representations of a collection of colors that use a mix of numeric values to represent each color. A different definition is found in [6] [7]. That's how we see color—hue, brightness, etc. [6]. Color models measure human-perceivable colors and combine values into primary colors. Different color spaces are better for digital video and picture compression techniques, TV monitoring and video cameras, scientific activity, and television broadcasts [8] [9]

[10]. Linear transforms can produce many color spaces from RGB, including YCbCr, NTSC, XYZ, and HSV, but RGB (red, green, blue) is used for TV monitors and video cameras [11] [12]. The YCbCr model is widely used in digital video and image compression schemes [13][14], but artists prefer the HIS (Hue, Intensity, and Saturation) and HSV (Hue, Saturation, and Value) spaces [15] [16], because they match how humans describe and interpret colors.

In the de-correlated color spaces YCbCr, YUV, NTSC, and YIQ, Y is luminance, I is cyan orange, and Q is purple-green [8]. Pixel colors are a mix of red, green, and blue [17] [18] [19]. The YCbCr model is utilized in digital video and picture compression schemes, the YUV model was widely used in Australian and European television transmissions. While the NTSC-named YIQ color space was used in North America, Japan, and elsewhere[8].

The XYZ color space is widely used in scientific work, and color descriptions in other color spaces are often related to their representation in this space. For image inpainting, the various color spaces are divided into two categories

according to their properties.

In the first category, each color channel represents all image information such as texture and structure in the image in addition to color. For example, in RGB space, R represents all information and red color while G and B channels are representing all information for green and blue colors, respectively. Thus, the most common color spaces in the first group is RGB. The color information in the second category is represented in two channels chrominance and luminance which have all information of texture and structure as seen in the color spaces of YCbCr, NTSC, HSV as well XYZ [20]. Colors help humans communicate with their species and daily objects. Colors should be represented numerically in a mathematical formula for device/computer storage and applications. Color models use Red, Green, and Blue to represent color space mathematically. The computer can simulate human hue and lightness [1].

Computer graphics, image processing, TV transmission, and computer vision use color modes. The color model uses mathematical functions to briefly convert light color coordinates into three color components [8]. The color model can be defined as the digital representation of possibly contained colors [21] [22], while [6] defines it as the way we recognize color through its hue and brightness [6]. Color models combine values to create primary colors[15]. Three- or four-color models are typical.

Color spaces vary by application [6]. Image processing applications divide color models into three types;

1. Device-oriented color models are dependent on a device's signal and are affected by the techniques used to create them [6] [4]. These versions are utilized in many applications that require color consistency with hardware tools [6], such as TVs [23] [24], and video systems [25] [26].
2. User-friendly color models: These models allow the user to describe and estimate what he sees after seeing the color [27] [28].
3. Device-free color models: The color model is unaffected by [27] [28], and the parameters produce the same hue regardless of device performance. Because visual data must pass through several hardware components, these color models aid network information transfer [6]. The image needed to be recovered utilizing the interior coating process because of the importance of color spaces in the application. This paper offered two coating models, The isotropic classic model and the RGB-proven improved model [29]. The two mathematical models applied to HSV, YCbCr, XYZ, and NTSC color spaces. Thus, the visual analysis evaluates inpainted images, while statistical measurements estimate their quality. The original and modified isotropic models estimate inpainted image quality using MSE, SSIM, and PSNR [30]. This work modifies the isotropic model-based inpainting to improve results

2. Mathematical Models

Used two mathematical models to recover the missing area

in the images, which are the isotropic model and modify the isotropic model.

2.1 Isotropic Model

Diffusion-based inpainting is the first model used to recover the damaged or missing part of the image by spreading information from the surrounding areas of the missing region at the pixel point [31]. However, isotropic diffusion is the second-order linear parabolic equation. Let $f \in L^2(\Omega)$ is an image and $D \subset \Omega$ is a missing information region from the original image; When u_t is Image derived over time (t). u is the inpainted image is given by the solution of the below equation[32]:

$$\begin{cases} u_t = \Delta u, & t \geq 0 \\ u(0, x, y) = 0. \end{cases} \dots(1)$$

In addition, u can be calculated from the solution of minimization functional for the squared total variation. The formula of the heat equation can be introduced as minimization energy functional as [33]:

$$\min_{u \in L^2(\Omega)} \{ \iint |\nabla u|^2 \, dx dy, \text{ such that } u = f \text{ in } \Omega \setminus D \} \dots(2)$$

Euler- Lagrange equation and gradient descent method are applied to the minimization functional 2, and we get

$$u_t = \Delta u \dots(3)$$

The solution of equation 1 or 3 with the Dirichlet boundary condition is used to recover the missing regions in the image. The explicit finite difference method (EFDm) is applied to find the solution of equation 1 or 3, which is imitative of the solution of the heat equation on the spatial (image) domain. This equation has studied the spreading of temperatures (information) within a period in all directions based on the boundary condition[34]. However, the spread in all directions will cause failure to recover edge construction of the missing area and appear blurred under the isotropic model (Eq.3). The diffusion term comes from the idea of propagating local information with smoothness constraints by analogy with some physical phenomena like heat propagation in physical structures [35]. Isotropic diffusion acts as low-pass linear filtering suppressing high frequencies in the image thus, it works to minimize these variations in all directions that in turn lead to appearing blurred close to edges and contours. More general formalisms using nonlinear PDEs are used for describing the physical and fluid dynamics phenomena to get better restoration of edges and more sharpness [16]

2.2 Modified Isotropic Model

The isotropic diffusion model is modified by adding more than one algebraic expression to reduce the blur of the large missing area and enhance the edge of restoration. Modified isotropic model (Eq.3) is modified by adding the first derivative of the missing area of the image [29]. The ability of the first derivative helps to build the edges and extend the isophote line, which improves the recovery of missing areas. The modified isotropic equation is written as follows:

$$u_t = \Delta u + \alpha u_x + \beta u_y, \quad t \geq 0 \dots(4)$$

Where u_x and u_y are the first derivatives of the image, the α and β are coefficients. Furthermore, the value of α and β play an important effect on the values of quality measures.

3. Proposed Method

First images converted from RGB to color spaces (XYZ, HSV, YCbCr, NTSC). When the isotropic model (Eq.3) and modified model (Eq.4) are applied on the missing region reconverted to the RGB. The image is then converted back to RGB color space using quality assessment to measure the completed algorithm for the image inpainted method is represented in the flow process below and the flowchart in Fig. (1(a)) and Fig.(1(b)).

3.1 Algorithm

1. Load a color image
2. Convert from RGB to color space.
3. Making the missing area by the researcher
4. Channels separation.
5. Using the equation to address the problems of the missing region.
6. Convert from color space to RGB.
7. Image quality assessment.

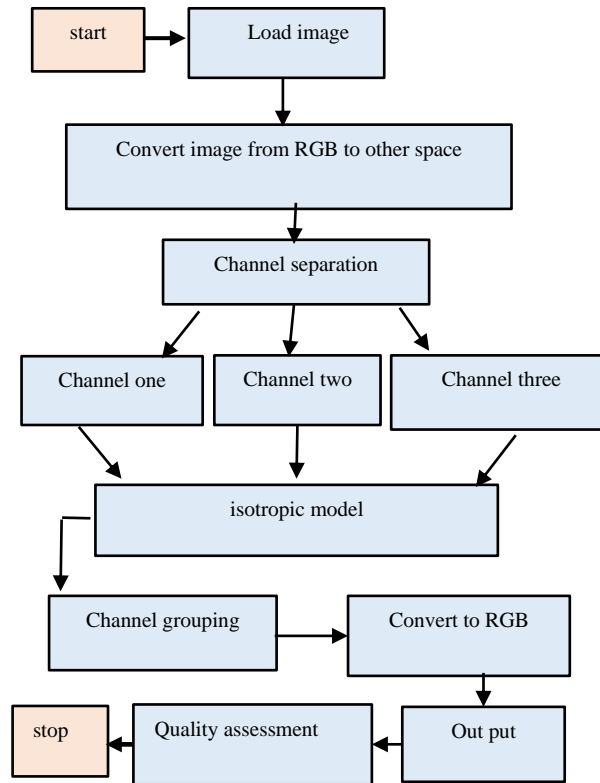


Figure.1(a): Flowchart of image inpainting algorithm by isotropic model

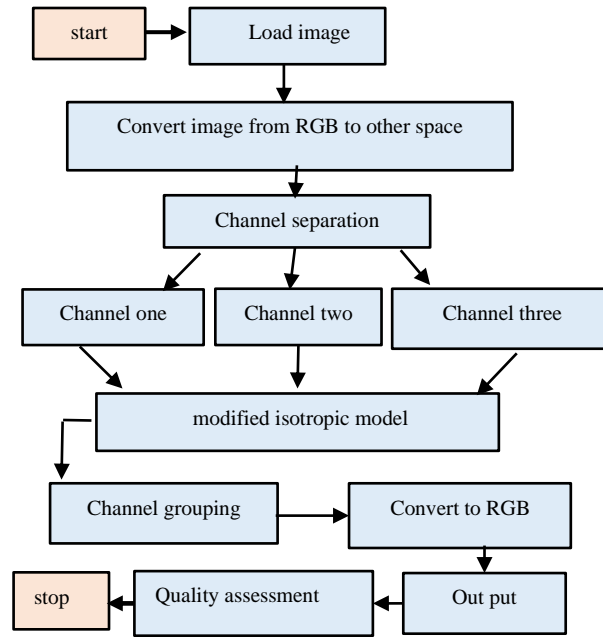


Figure.1(b): Flowchart of image inpainting algorithm by modified isotropic model

4. Experimental Results

The experiments in this paper include applying the isotropic model (Eq.3) and the modified isotropic model (Eq.4). The experiments were tested on different 100 natural images selected from Berkeley Segmentation Dataset 300

(BSDS300) [36], (See Fig.2). And for four shapes of the mask (missing area) marked by the user, all masks are regular shapes, and had different size and type, including the square, the narrow rectangle, the wide rectangle, the horizontal and vertical with different locations from the image. (See Fig.3).



Figure. 2: Example of natural images

The Matlab (R2018a) programming was used to test the modified model on the selected standard natural images.

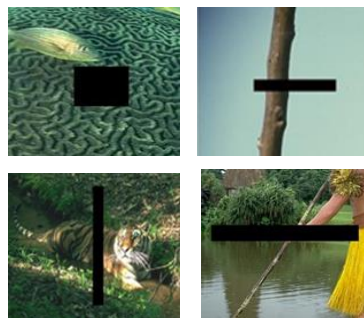


Figure 3: Type of masks (missing area)

4.1 Experimental Results of Different Color Spaces

In these experiments, the isotropic model (Eq. 3) and the modified model (Eq.4) were applied to four different color spaces YCbCr, NTSC, XYZ, and HSV to study the behavior of the two models in these color spaces and their ability to recover missing areas in these color spaces and to compare the results of the experiments visually and statistically obtained using the MSE, PSNR, and SSIM quality

assessment. Figure 4 shows the original images. Figure 4 shows the original images. Figure 5 shows the results obtained by applying the isotropic model (Eq.3) for the four-color spaces referred to earlier and with the four forms of masks (missing regions) shown in the figure 3. Figure 6 shows the results of applying the modified isotropic model (Eq. 4) to recover the missing region



Figure 4: Original images

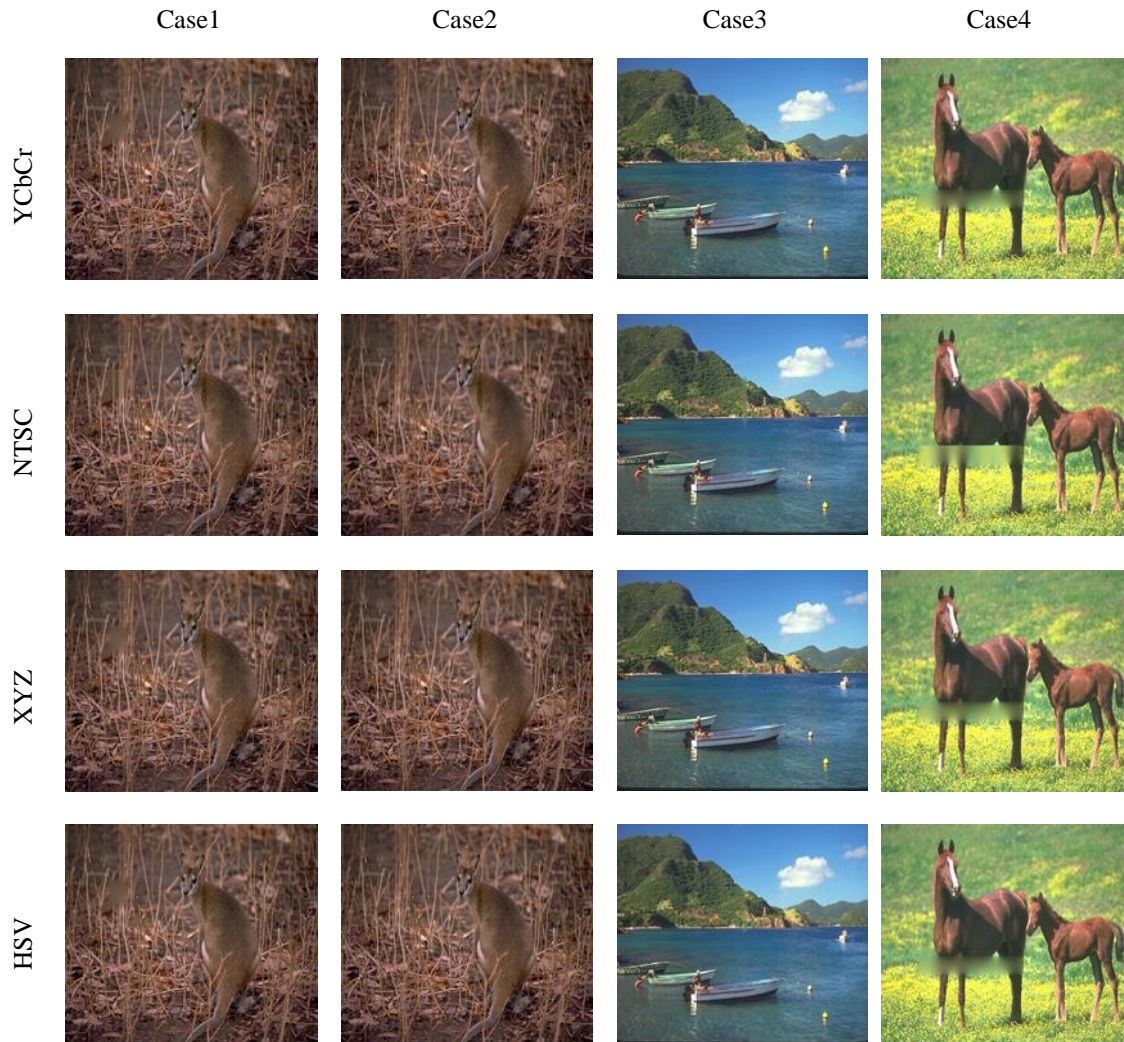


Figure. 5: Image inpainted in different color spaces by using isotropic model (Eq.3)

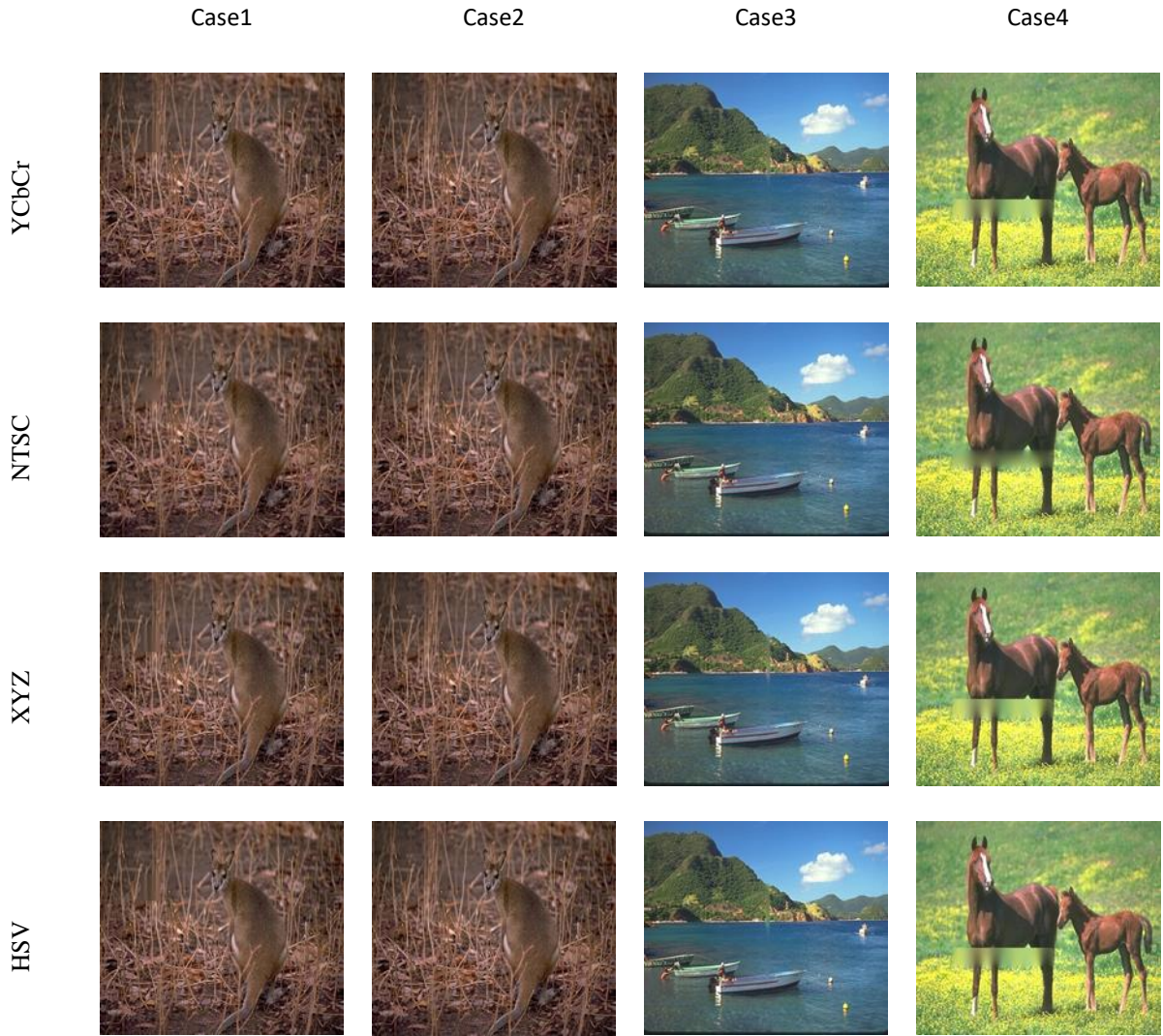


Figure. 6: Image inpainted in different color spaces by using a modified isotropic model (Eq.4).

Statistical quality measures such as MSE, PSNR and SSIM and execution time are measured to evaluate the quality of the inpainting of the missing areas in the image and to compare the effectiveness of the two models used in painting on different areas and different color spaces. The values are presented in the tables below.

Whereas table 1 shows the results of applying the classical isotropic and modified models on the square missing region (Case 1) by. The average of MSE, PSNR, and SSIM values

of 100 images using classical isotropic (Eq.3) and the modified isotropic (Eq.4) models. The average of consumed time values is calculated using both classical isotropic model (Eq.3) and modified isotropic model (Eq.4). The results were as follows: the better value of MSE was when using the XYZ space and the better value of PSNR when using the NTSC space and the better value of SSIM in YCbCr space when using the modified model and classic isotropic model (Eq.3).

Table 1: Image quality assessment in case 1

Models	Spaces	MSE	PSNR	SSIM	Time (S)
Isotropic Model	YCbCr	23.930	41.625	0.852	10.624
	NTSC	0.051	70.317	0.181	10.434
	XYZ	0.045	65.127	0.080	11.214
	HSV	0.105	59.212	0.127	11.153
Modify Isotropic Model	YCbCr	29.327	39.593	0.792	1.095
	NTSC	0.058	70.051	0.167	1.106
	XYZ	0.056	64.797	0.076	1.338
	HSV	0.123	58.651	0.113	1.126

While table 2 shows the results of applying the classical isotropic and modified models on small and narrow rectangle shapes (Case 2) in the different color spaces. The results were as follows: the highest value of MSE was when using the YCbCr space and the lowest value was when using the XYZ space. The lowest MSE values appeared in XYZ space using

both classical isotropic and modified models, the best value of PSNR in NTSC space was used, the isotropic model. While the best values of the SSIM whether using the classical isotropic model (Eq.3) or the modified model (Eq.4) appeared in the YCbCr color space.

Table 2: Image quality assessment in case 2

Models	Spaces	MSE	PSNR	SSIM	Time (S)
Isotropic Model	YCbCr	8.417	47.131	0.922	1.524
	NTSC	0.037	71.404	0.206	1.574
	XYZ	0.033	67.402	0.201	1.285
	HSV	0.101	60.132	0.144	1.289
Modify Isotropic Model	YCbCr	11.551	45.274	0.899	0.672
	NTSC	0.038	71.393	0.206	0.656
	XYZ	0.035	67.347	0.200	0.981
	HSV	0.103	60.073	0.144	1.047

Table 3 shows the results of applying the classical isotropic and modified models on the narrow rectangular region extending vertically (Case 3) on the different color spaces. The results were as follows: the less value of MSE was for XYZ space is equal (0.031). But the value of SSIM has the

best value in YCbCr space is equal (0.922), while, the best results for PSNR were in NTSC space by using the classical isotropic model (Eq.3) and modified isotropic model (Eq.4).

Table 3: Image quality assessment in case 3

Models	Spaces	MSE	PSNR	SSIM	Time (S)
Isotropic Model	YCbCr	11.541	43.545	0.888	2.401
	NTSC	0.044	69.568	0.157	1.229
	XYZ	0.031	65.303	0.086	1.354
	HSV	0.105	59.027	0.116	1.262
Modify Isotropic Model	YCbCr	18.569	40.118	0.788	15.018
	NTSC	0.048	69.427	0.154	10.746
	XYZ	0.034	65.112	0.084	11.873
	HSV	0.118	58.661	0.097	11.556

Table 4 shows the results of applying the classical isotropic and modified models on large missing areas (Case 4) in the different color spaces. The results were as follows: the best results of MSE in XYZ space, PSNR in NTSC space, and SSIM appeared in YCbCr space using the modified model and classical isotropic model (Eq.3). The modified model (Eq.4) consumes a little more time than the classical isotropic model by reconstructing the missing regions for all missing cases. In this experiment, the classical isotropic and modified models have applied different color spaces, and the 100 images have been selected from [22] in terms of the size of the missing region and the quantity of texture in the surrounding areas of missing regions. These models have been applied to four cases of missing regions; these cases have been used based on the size of missing regions. The evaluation of the analysis quality indicates when the missing region was narrow and small a rectangle, the MES was the lowest compared to other cases when using the isotropic model and when using the modified equation in

YCbCr. However, the MES decreased values when the isotropic equation of the model and modify isotropic model are used for inpainting the missing region, respectively. Furthermore, the best average PSNR value was obtained for case two when the original equation and the modified one were applied especially in NTSC space. The SSIM is an important indicator of the similarity between the original image and the inpainted one. The obtained results confirmed that the small missing area in case two led to getting better SSIM than other cases in both models and the YCbCr space. However, modified model appeared SSIM value less than Isotropic Model (Eq.3) for YCbCr space. When comparing the statistical and visual results in the case of applying the two models to the RGB space, see[29], with the results of this article, it is clear that the ability of the improved model (Eq.4) to restore the missing areas is better than all other spaces. The improvement increases whenever the area is small and narrow, and the amount of texture around the missing area does not differ in quality and quantity from the texture inside the missing area.

Table 4: Image quality assessment in case 4

Models	Spaces	MSE	PSNR	SSIM	Time (S)
Isotropic Model	YCbCr	38.881	0.816	61.780	38.881
	NTSC	68.982	0.153	40.522	68.982
	XYZ	64.133	0.065	43.545	64.133
	HSV	58.606	0.110	46.046	58.606
Modify Isotropic Model	YCbCr	24.864	38.540	0.797	9.084
	NTSC	0.0592	68.792	0.157	7.701
	XYZ	0.0442	63.924	0.069	8.328
	HSV	0.133	58.218	0.111	8.033

6. Conclusions

The isotropic model and modified isotropic model were used in the process of restoring the missing regions in the images. It was applied to a set of different images and shapes of the missing areas. It was applied to more than one color space to find out which models have the best ability to restore lost areas and inpaint. The results show that NTSC space is considered the best space where MSE is lower and PSNR is higher. It was also concluded that the results are better when the missing area is small and the texture around the missing area is not much different from the texture inside the missing area in quantity and quality, but the inpainted area is blurry when the missing area is large. The reason for this may be attributed to the dissemination of information in all directions, and this is one of the characteristics of the isotropic model.

References

- [1] T. B. Taha, T. Nurtayeva, S. A. Arif, and A. S. Jamal, "Partial Differential Equations and Digital Image Processing: A Review," in 2022 8th International Engineering Conference on Sustainable Technology and Development (IEC), 2022, pp. 235–240.
- [2] S. J. Li and Z. A. Yao, "Image inpainting algorithm based on partial differential equation technique," *Imaging Sci. J.*, vol. 61, no. 3, pp. 292–300, 2013.
- [3] D. R. Ibrahim, J. Sen Teh, and R. Abdullah, "An overview of visual cryptography techniques," *Multimed. Tools Appl.*, vol. 80, pp. 31927–31952, 2021.
- [4] S. Jardim, J. António, and C. Mora, "Image thresholding approaches for medical image segmentation-short literature review," *Procedia Comput. Sci.*, vol. 219, pp. 1485–1492, 2023.
- [5] R. C. Gonzalez, R. E. Woods, and B. R. Masters, "Digital Image Processing, Third Edition," *J. Biomed. Opt.*, vol. 14, no. 2, p. 029901, 2009, doi: 10.1117/1.3115362.
- [6] D. Wu and D.-W. Sun, "Colour measurements by computer vision for food quality control—A review," *Trends Food Sci. Technol.*, vol. 29, no. 1, pp. 5–20, 2013.
- [7] A. Ford and A. Roberts, "Colour space conversions," *Westminster Univ. London*, vol. 1998, pp. 1–31, 1998.
- [8] M. Ramesh and K. Mahesh, "A performance analysis of pre-trained neural network and design of CNN for sports video classification," in 2020 International Conference on Communication and Signal Processing (ICCSP), 2020, pp. 213–216.
- [9] K. Shankar, K. Mahesh, and K. Kuppusamy, "Analyzing Image Quality via Color Spaces," *image. In*, vol. 1, no. 1, 2014.
- [10] A. Bansal, R. Bajpai, and J. P. Saini, "Simulation of image enhancement techniques using Matlab," in First Asia International Conference on Modelling & Simulation (AMS'07), 2007, pp. 296–301.
- [11] G. K. Ijamaru et al., "Image processing system using MATLAB-based analytics," *Bull. Electr. Eng. Informatics*, vol. 10, no. 5, pp. 2566–2577, 2021.
- [12] K. Kaur and M. M. Kaur, "Case Study of Color Model of Image Processing," *Int. J. Comput. Eng. Technol.*, vol. 6, no. 12, pp. 65–71, 2015.
- [13] M. Serouart et al., "SegVeg: Segmenting RGB images into green and senescent vegetation by combining deep and shallow methods," *Plant Phenomics*, vol. 2022, 2022.
- [14] W. Burger and M. J. Burge, *Principles of digital image processing: fundamental techniques*. Springer Science & Business Media, 2010.
- [15] U. Rahamathunnisa, B. C. Chetty, and A. C. King, "A survey on fault detection techniques in different machines—an image processing approach," *Int. J. Civ. Eng. Technol.*, vol. 8, no. 9, 2017.
- [16] G. H. Joblove and D. Greenberg, "Color spaces for computer graphics," in *Proceedings of the 5th annual conference on Computer graphics and interactive techniques*, 1978, pp. 20–25.
- [17] F. Bianconi, A. Fernández, F. Smeraldi, and G. Pascoletti, "Colour and texture descriptors for visual recognition: A historical overview," *J. Imaging*, vol. 7, no. 11, p. 245, 2021.
- [18] W. Burger, M. J. Burge, M. J. Burge, and M. J. Burge, *Principles of digital image processing*, vol. 111. Springer, 2009.
- [19] J. Bigun, *Vision with direction*. Springer, 2006.
- [20] Z. A. AbdulKareem, *Numerical Solutions Analysis of Image Inpainting AlgorithmsBased Partial Differential Equations*. University of Basrah, 2023.
- [21] M. S. Woolf, L. M. Dignan, A. T. Scott, and J. P. Landers, "Digital postprocessing and image segmentation for objective analysis of colorimetric reactions," *Nat. Protoc.*, vol. 16, no. 1, pp. 218–238, 2021.
- [22] N. A. Ibraheem, M. M. Hasan, R. Z. Khan, and P. K. Mishra, "Understanding color models: a review," *ARPN J. Sci. Technol.*, vol. 2, no. 3, pp. 265–275, 2012.
- [23] M. Momtaz Dargahi, A. Khaloo, and D. Lattanzi, "Color-space analytics for damage detection in 3D point clouds," *Struct. Infrastruct. Eng.*, vol. 18, no. 6, pp. 775–788, 2022.
- [24] R. J. Rasras, E. I. M. M. El, and D. E. Skopin, "Developing a new color model for image analysis and processing," *Comput. Sci. Inf. Syst.*, vol. 4, no. 1, pp. 43–55, 2007.
- [25] M. Domino et al., "Selection of image texture analysis and color model in the advanced image processing of thermal images of horses following exercise," *Animals*, vol. 12, no. 4, p. 444, 2022.
- [26] C.-Y. Wen and C.-M. Chou, "Color image models and its applications to document examination," *Forensic Sci. J.*, vol. 3, no. 1, pp. 23–32, 2004.
- [27] S. Vijh, M. Saraswat, and S. Kumar, "A new complete color normalization method for H&E stained histopathological images," *Appl. Intell.*, pp. 1–14, 2021.
- [28] K. Plataniotis and A. N. Venetsanopoulos, *Color image processing and applications*. Springer Science & Business Media, 2000.
- [29] Z. A. A. Kareem and A. K. Al-Jaberi, "A Novel Image Inpainting Technique Based on Isotropic Diffusion," *Basrah J. Sci.*, vol. 40, no. 2, pp. 289–305, 2022.
- [30] A. Halim and B. V. R. Kumar, "An anisotropic PDE model for image inpainting," *Comput. Math. with Appl.*, vol. 79, no. 9, pp. 2701–2721, 2020.
- [31] K. R. Patel, L. Jain, and A. G. Patel, "Image inpainting—a review of the underlying different algorithms and comparative study of the inpainting techniques," *Int. J. Comput. Appl.*, vol. 118, no. 10, 2015.
- [32] C. Guillemot and O. Le Meur, "Image inpainting: Overview and recent advances," *IEEE Signal Process. Mag.*, vol. 31, no. 1, pp. 127–144, 2013.
- [33] A. K. Al-Jaberi and E. M. Hameed, "A Review of PDE Based Local Inpainting Methods," in *Journal of Physics: Conference Series*, 2021, vol. 1818, no. 1, p. 12149.
- [34] G. Aubert, P. Kornprobst, and G. Aubert, *Mathematical problems in image processing: partial differential equations and the calculus of variations*, vol. 147. Springer, 2006.
- [35] S. Masnou and J.-M. Morel, "Level lines based disocclusion," in *Proceedings 1998 International Conference on Image Processing. ICIP98 (Cat. No. 98CB36269)*, 1998, pp. 259–263.
- [36] P. Arbelaez, C. Fowlkes, and D. Martin, "The Berkeley segmentation dataset and benchmark," *Comput. Sci. Dep. Berkeley Univ.* Available <http://www.eecs.berkeley.edu/Research/Projects/CS/vision/bsds>, 2007.

نموذج جديد للطلاء الداخلي للصورة لفضاءات لونية مختلفة

احمد كاظم الجابري
قسم الرياضيات، كلية التربية
للعلوم الصرفة، جامعة البصرة،
البصرة، العراق

زينب علي عبد الكريم
قسم الرياضيات، كلية العلوم،
جامعة البصرة، البصرة، العراق

ahmed.shanan@uobasrah.edu.iq zaynab.eali.sci@uobasrah.edu.iq
تاريخ القبول: 11/7/2023 تاريخ الاستلام: 29/3/2023

الملخص

طبقت الطريقة المطورة حديثاً لطلاء المنطقة المفقودة في الصور الرقمية التي تستند إلى نموذج الخواص على مجموعة متنوعة من الفضاءات اللونية، بما في ذلك فضاءات الألوان XYZ و YCbCr و NTSC و HSV. تم إجراء الاختبارات باستخدام الأفعنة التي ابتكرها الباحث بناءً على الصور الأصلية (الواضحة)؛ تختلف هذه الأفعنة من حيث الحجم والشكل. من أجل تقييم جودة الرسم الداخلي للصورة، يتم استخدام مقاييس الجودة الإحصائية مثل MSE (متوسط الخطأ المربع) و PSNR (إشارة الذروة إلى نسبة الضوضاء) و SSIM (مؤشر التشابه الهيكلي). كان أداء هذه الطريقة متفوقاً على أحدث معادلات PDEs (المعادلات التفاضلية الجزئية) في طرق الطلاء الداخلي القائمة على PDE؛ فضاءات لونية.